GEOPHYSICS, VOL. 57, NO. 10 (OCTOBER 1992); P. 1334–1345, 20 FIGS.

Optimum seismic illumination of hydrocarbon reservoirs

W. E. A. Rietveld*, A. J. Berkhout*, and C. P. A. Wapenaar*

ABSTRACT

A method is proposed for the design and application of a wave theory-based synthesis operator, which combines shot records (2-D or 3-D) for the illumination of a specific part of the subsurface (target, reservoir) with a predefined source wavefield.

After application of the synthesis operator to the surface data, the procedure is completed by downward extrapolation of the receivers. The output simulates a seismic experiment at the target, carried out with an optimum source wavefield. These data can be further processed by migration and/or inversion.

The main advantage of the proposed method is that control of the source wavefield is put at the target, in contrast with the conventional wave stack procedures, where control of the source wavefield is put at the surface. Moreover, the proposed method allows true amplitude, three-dimensional (3-D), prestack migration that can be economically handled on the current generation of supercomputers.

INTRODUCTION

During the last few years, the acquisition of seismic measurements has shifted from two-dimensional (2-D) to three-dimensional (3-D) surveys. Unfortunately, the total amount of data obtained from these 3-D surveys is so large, that full prestack imaging in a true 3-D sense is still not feasible, even on current supercomputers.

We propose an efficient as well as accurate procedure that enables us to illuminate a specific part of the subsurface (target, reservoir) in a predefined way. This is done by redefining the shot records at the surface using a wave theory-based synthesis operator. This synthesis operator is defined by the illumination requirements and by the macro properties of the subsurface (overlying the reservoir).

Application of this synthesis operator simulates one seismic experiment with one areal source. Hence, the synthesis process reduces the total amount of data to one so-called areal shot record. The effect of the synthesized areal source at the surface is a desired downward traveling source wavefield at a (potential) reservoir, generally with a unit amplitude and a specific shape, e.g., to simulate normal or plane wave incidence. Hence, after the synthesis, downward extrapolation of the receivers needs to be done only on the areal shot record, yielding the response of the reservoir at the top of the reservoir, due to the prespecified source wavefield at the top of the reservoir. Next, imaging and/or inversion can start inside the reservoir.

History

The synthesis of an areal seismic source from the individual field sources is not new. Already, Taner (1976) proposed to synthesize plane wave sources at the surface by stacking traces in a common receiver gather. A similar process was discussed by Schultz and Claerbout (1978). It is important to realize that with the procedures of Taner (1976) and Schultz and Claerbout (1978) the control of the source wavefield is put at the surface. However, it is argued in this paper that the control of the source wavefield should not be put at the surface, but should be put at the target. Recently, Berkhout (1992) introduced the concept of areal shot record technology in the open literature. Optimum illumination can be seen as a special version of areal shot record migration.

Outline

We start with a brief description of the forward matrix model for reflection measurements. From this forward model, a general prestack redatuming scheme and the scheme for optimum illumination are derived. It is shown theoretically and with an example that the proposed procedure of synthesizing shot records at the surface followed by extrapolation to the top of the target (reservoir) is fully equivalent to the computationally expensive method of extrapolating the individual shot records to the top of the target, followed by synthesis at the target. Finally it is shown that the method also holds for incomplete data-acquisition grids.

Manuscript received by the Editor April 10, 1991; revised manuscript received March 30, 1992.
*Laboratory of Seismics and Acoustics, Delft University of Technology, P. O. Box 5046, 2600 GA Delft, The Netherlands.

FORWARD MODEL FOR REFLECTION MEASUREMENTS

In practice seismic measurements are always discrete in time and space. Consequently, imaging is always a discrete process and the theory should be discrete. Therefore, our forward model for reflection measurements is presented as a discrete model (Berkhout, 1985).

For linear wave theory in a time-invariant medium, the imaging problem may be described in the temporal frequency domain without any loss of information. Moreover, as our recording has a finite duration (T) we only need to consider a finite number of frequencies (N) per seismic trace, where

$$N = (f_{\max} - f_{\min})T, \tag{1}$$

$f_{\max} - f_{\min}$ being the temporal frequency range of interest. A typical number for N equals 250.

Taking into account the discrete property on the one hand and the allowed representation by independent frequency components on the other hand, vectors and matrices are preeminently suited for the mathematical description of recorded seismic data. For instance, considering one shot record, one element of the so-called measurement vector $\mathbf{P}(z_0)$ contains the complex number (defining amplitude and phase for the Fourier component under consideration) related to the recorded signal at one location of the acquisition plane $z = z_0$ (one detector position).

If the vector $\mathbf{S}^+(z_0)$ represents one Fourier component of the downward traveling source wavefield at the data acquisition surface $z = z_0$, then we may write:

$$\mathbf{S}^+(z_m) = \underset{\sim}{\mathbf{W}}^+(z_m, z_0)\mathbf{S}^+(z_0), \tag{2}$$

where $\mathbf{S}^+(z_m)$ is the monochromatic downward traveling source wavefield at depth level z_m and $\underset{\sim}{\mathbf{W}}^+(z_m, z_0)$ represents the downward propagation operator from z_0 to z_m. Operator $\underset{\sim}{\mathbf{W}}^+$ is represented by a complex-valued matrix, where each column equals one Fourier component of the response at depth level z_m due to one dipole at the surface. Note that for homogeneous media $\underset{\sim}{\mathbf{W}}^+$ becomes a convolution matrix.

At depth level z_m, reflection occurs. For each Fourier component, reflection may be described by a general linear operator $\underset{\sim}{\mathbf{R}}(z_m)$,

$$\mathbf{P}_m^-(z_m) = \underset{\sim}{\mathbf{R}}(z_m)\mathbf{S}^+(z_m), \tag{3}$$

where $\mathbf{P}_m^-(z_m)$ is the monochromatic upward traveling reflected wavefield at depth level z_m due to the inhomogeneities at depth level z_m only. Reflection operator $\underset{\sim}{\mathbf{R}}(z_m)$ represents a matrix, where each row describes the angle dependent reflection property of each grid point at z_m. If there is no angle dependence, $\underset{\sim}{\mathbf{R}}(z_m)$ is a diagonal matrix with angle independent reflection coefficients.

Finally, the reflected wavefield at z_m travels up to the surface,

$$\mathbf{P}_m^-(z_0) = \underset{\sim}{\mathbf{W}}^-(z_0, z_m)\mathbf{P}_m^-(z_m), \tag{4}$$

where $\mathbf{P}_m^-(z_0)$ is one Fourier component of the reflected wavefield at data acquisition surface z_0 and $\underset{\sim}{\mathbf{W}}^-(z_0, z_m)$ equals the upward propagation operator from z_m to z_0. Each column of $\underset{\sim}{\mathbf{W}}^-$ equals one Fourier component of the response at z_0 due to one dipole at depth level z_m.

Equations (2), (3), and (4) may now be combined into one matrix equation for the reflection response (Figure 1a):

$$\begin{aligned}
\mathbf{P}^-(z_0) &= \sum_{m=1}^{M} \mathbf{P}_m^-(z_0) \\
&= \sum_{m=1}^{M} \underset{\sim}{\mathbf{W}}^-(z_0, z_m)\mathbf{P}_m^-(z_m) \\
&= \sum_{m=1}^{M} \underset{\sim}{\mathbf{W}}^-(z_0, z_m)\underset{\sim}{\mathbf{R}}(z_m)\mathbf{S}^+(z_m) \\
&= \left[\sum_{m=1}^{M} \underset{\sim}{\mathbf{W}}^-(z_0, z_m)\underset{\sim}{\mathbf{R}}(z_m)\underset{\sim}{\mathbf{W}}^+(z_m, z_0)\right]\mathbf{S}^+(z_0)
\end{aligned} \tag{5a}$$

or, for a continuous formulation in z,

$$\mathbf{P}^-(z_0) = \int_{z_0}^{\infty} [\underset{\sim}{\mathbf{W}}^-(z_0, z)\underset{\sim}{R}(z)\underset{\sim}{\mathbf{W}}^+(z, z_0)\, dz]\mathbf{S}^+(z_0). \tag{5b}$$

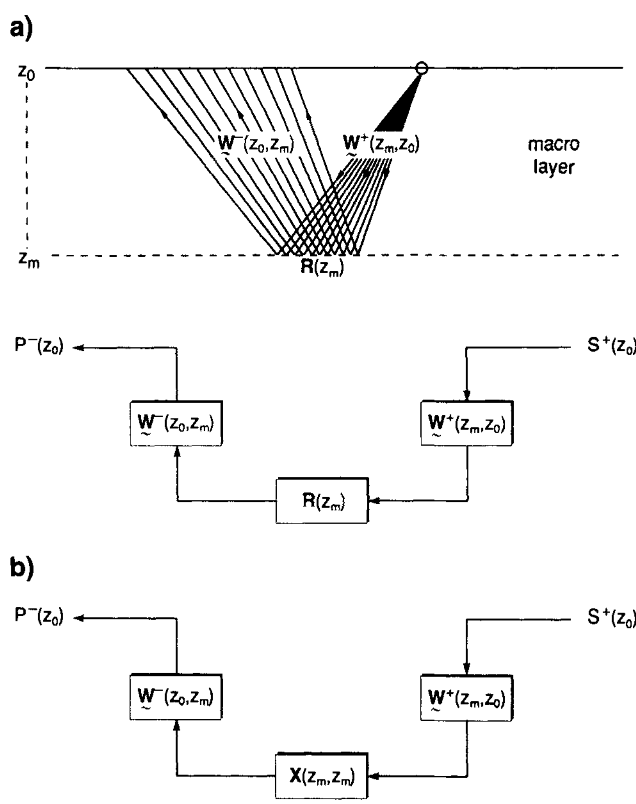

FIG. 1. (a) Propagation and reflection for one point source and one reflecting depth level (z_m), ignoring the reflectivity of the surface (z_0). (b) Response at the reflection-free surface ($z = z_0$) due to reflection in half-space $z \geq z_m$.

For further details the reader is referred to Berkhout (1985, chapter VI).

If we define the half-space reflection operator at depth level z_m due to inhomogeneities at $z \geq z_m$ by matrix $\underset{\sim}{\mathbf{X}}(z_m, z_m)$, then it follows from equation (5a) that we may write:

$$\underset{\sim}{\mathbf{X}}(z_m, z_m) = \sum_{n=m}^{M} \underset{\sim}{\mathbf{W}}^-(z_m, z_n)\underset{\sim}{\mathbf{R}}(z_n)\underset{\sim}{\mathbf{W}}^+(z_n, z_m). \tag{6}$$

The response of half-space $z \geq z_m$ at the surface can be formulated as (Figure 1b):

$$\mathbf{P}^-(z_0) = [\underset{\sim}{\mathbf{W}}^-(z_0, z_m)\underset{\sim}{\mathbf{X}}(z_m, z_m)\underset{\sim}{\mathbf{W}}^+(z_m, z_0)]\mathbf{S}^+(z_0) \tag{7a}$$

or

$$\mathbf{P}^-(z_0) = \underset{\sim}{\mathbf{X}}(z_0, z_0)\mathbf{S}^+(z_0) \tag{7b}$$

with

$$\underset{\sim}{\mathbf{X}}(z_0, z_0) = \underset{\sim}{\mathbf{W}}^-(z_0, z_m)\underset{\sim}{\mathbf{X}}(z_m, z_m)\underset{\sim}{\mathbf{W}}^+(z_m, z_0), \tag{7c}$$

where the effect of the surface has already been eliminated by preprocessing (Verschuur et al., 1992).

Note that matrix element $X_{ij}(z_m, z_m)$ may be considered as one Fourier component of the reflection response at position i on surface $z = z_m$, due to a unit dipole source at position j on the same surface ($z = z_m$).

The multiexperiment formulation of equation (7a) yields:

$$\underset{\sim}{\mathbf{P}}^-(z_0) = [\underset{\sim}{\mathbf{W}}^-(z_0, z_m)\underset{\sim}{\mathbf{X}}(z_m, z_m)\underset{\sim}{\mathbf{W}}^+(z_m, z_0)]\underset{\sim}{\mathbf{S}}^+(z_0), \tag{7d}$$

where one column of source matrix $\underset{\sim}{\mathbf{S}}^+(z_0)$ defines the induced source function of one monochromatic experiment and the related column of measurement matrix $\underset{\sim}{\mathbf{P}}^-(z_0)$ defines the monochromatic versions of the measured signals of that experiment.

So far we have not discussed the effect of multiple scattering and the interaction of the sources and receivers with the free surface. However, in our stepwise inversion scheme, as e.g., described in Berkhout and Wapenaar (1990), the interaction of the sources and receivers with the free surface, together with the multiples related to the free surface are removed by a surface-related preprocessing step. Therefore, the data after preprocessing may be described by the simplified forward model of equations (7), where $\underset{\sim}{\mathbf{W}}^+$ and $\underset{\sim}{\mathbf{W}}^-$ may still include internal multiple scattering.

In the following, we will concentrate on the redatuming of prestack data to obtain the response of the target area, i.e., we transform $\underset{\sim}{\mathbf{X}}(z_0, z_0)$ to $\underset{\sim}{\mathbf{X}}(z_m, z_m)$.

PRESTACK REDATUMING

The purpose of redatuming is to transform the data in such a way that the acquisition level is transported from the surface to another level ("datum") somewhere in the subsurface (Figure 2). Such a processing scheme has been described in Berryhill (1984). From our forward matrix model, as described in the previous section, it is simple to construct the formulas for such a prestack redatuming scheme.

Removing the propagation effects from the forward model [equation (7c)] means applying the inverse of the propagation operators $\underset{\sim}{\mathbf{W}}^+(z_m, z_0)$ and $\underset{\sim}{\mathbf{W}}^-(z_0, z_m)$:

$$\underset{\sim}{\mathbf{X}}(z_m, z_m) = \underset{\sim}{\mathbf{F}}^-(z_m, z_0)\underset{\sim}{\mathbf{X}}(z_0, z_0)\underset{\sim}{\mathbf{F}}^+(z_0, z_m), \tag{8}$$

where

$$\underset{\sim}{\mathbf{F}}^+(z_0, z_m) = [\underset{\sim}{\mathbf{W}}^+(z_m, z_0)]^{-1} \approx [\underset{\sim}{\mathbf{W}}^-(z_0, z_m)]^*$$

$$\underset{\sim}{\mathbf{F}}^-(z_m, z_0) = [\underset{\sim}{\mathbf{W}}^-(z_0, z_m)]^{-1} \approx [\underset{\sim}{\mathbf{W}}^+(z_m, z_0)]^*,$$

* denoting that the complex conjugated version should be taken.

Equation (8) gives the general scheme for prestack redatuming (Berkhout, 1985, chapter VII).

Redatuming as described by equation (8) can be carried out in a two-step way: first the extrapolation of the receivers to the target:

$$\underset{\sim}{\mathbf{X}}(z_m, z_0) = \underset{\sim}{\mathbf{F}}^-(z_m, z_0)\underset{\sim}{\mathbf{X}}(z_0, z_0), \tag{9a}$$

followed by the extrapolation of the sources:

$$\underset{\sim}{\mathbf{X}}(z_m, z_m) = \underset{\sim}{\mathbf{X}}(z_m, z_0)\underset{\sim}{\mathbf{F}}^+(z_0, z_m). \tag{9b}$$

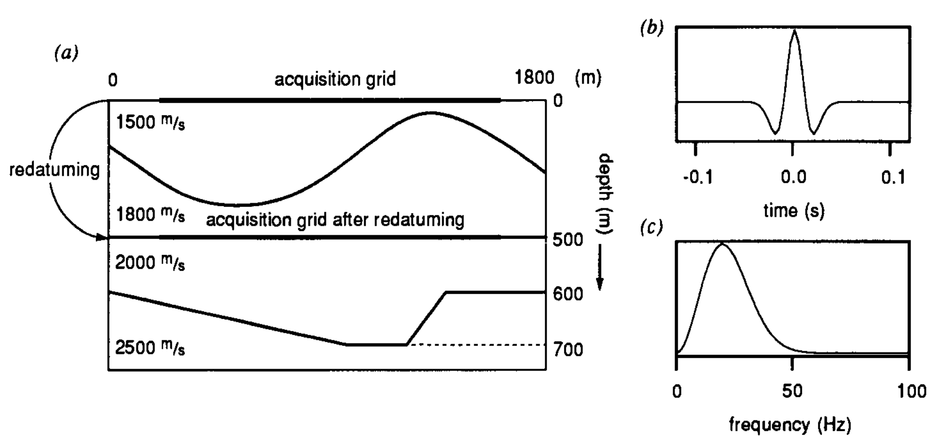

FIG. 2. The subsurface model used for the example (a). Indicated is the principle of redatuming. On the right-hand side the wavelet used (b) and its spectrum (c) are shown.

Equations (9a) and (9b) describe in a concise way redatuming according to the well-known SG method (Shot-Geophone method). The detailed algorithm follows directly from the way matrices should be multiplied.

For practical applications redatuming according to equations (9a) and (9b) may not be the most efficient solution. For 3-D applications in particular, it involves a cumbersome data reordering process in between the two steps. It is possible to derive an alternative scheme where the redatuming is performed per shot record (see e.g., Wapenaar and Berkhout, 1989, chapter XI), thereby avoiding the data reordering process and allowing irregular shot positions.

Although from a data handling point of view the shot record method is much simpler than the SG method, still a lot of computational effort is involved, particularly in 3-D. We will show that by synthesizing the shot records into one areal shot record, the total amount of data reduces significantly and a considerable speedup of the redatuming process is achieved without losing any accuracy.

OPTIMUM ILLUMINATION

In this section, we will focus on the theoretical aspects of the optimum illumination process, and we will illustrate the principle with an example. First a short discussion on the synthesis of shot records at the surface will be given. This is followed by the description of the design of the synthesis operator, defining the way to combine the shot records at the surface to obtain the desired illumination of the target. Then the application of the synthesis operator to the shot records is described. Finally the comparison is made between "synthesis at the surface, followed by redatuming to the target" and "redatuming to the target, followed by synthesis at the target."

For the example, consider the subsurface model as depicted in Figure 2, where the acquisition spread consists of 128 shots and 128 receivers in a fixed spread configuration with a spacing of 12 m. A zero-phase Ricker wavelet was used as shown in Figure 2. The modeling for the example was done by a 2-D, acoustic, finite-difference scheme.

The synthesis of shot records at the surface

Considering the forward model as derived in a previous section, the incident wavefield at depth level z_m is given by (see also Figure 3):

$$\mathbf{S}^+(z_m) = \underset{\sim}{\mathbf{W}}^+(z_m, z_0)\mathbf{S}^+(z_0), \tag{10a}$$

or for a range of experiments:

$$\underset{\sim}{\mathbf{S}}^+(z_m) = \underset{\sim}{\mathbf{W}}^+(z_m, z_0)\underset{\sim}{\mathbf{S}}^+(z_0). \tag{10b}$$

We now synthesize an areal source at the surface z_0 from the differently positioned local sources that are related to the different experiments. If $\mathbf{\Gamma}^+(z_0)$ is the complex-valued synthesis operator, the synthesized wavefield at the surface z_0 equals:

$$\mathbf{S}^+_{\text{syn}}(z_0) = \underset{\sim}{\mathbf{S}}^+(z_0)\mathbf{\Gamma}^+(z_0), \tag{11}$$

and the incident wavefield at depth level z_m due to this areal source equals:

$$\mathbf{S}^+_{\text{syn}}(z_m) = \underset{\sim}{\mathbf{W}}^+(z_m, z_0)\underset{\sim}{\mathbf{S}}^+(z_0)\mathbf{\Gamma}^+(z_0). \tag{12}$$

For the special situation:

$$\mathbf{\Gamma}^+(z_0) = (1, 1, \ldots, 1)^T, \tag{13a}$$

the areal source wavefield at the surface z_0 will be a horizontal plane wave. Figure 4 shows the propagation of a horizontal plane wave through an inhomogeneous subsurface. Note that the incident wavefield at z_m is not a plane wave due to the propagation distortion of the overburden. The synthesis operator as given by equation (13a) is characteristic for conventional synthesis methods. For slant plane-wave stacking procedures the synthesis operator should be written as:

$$\mathbf{\Gamma}^+(z_0) = (e^{-j\omega p x_1}, e^{-j\omega p x_2}, \ldots, e^{-j\omega p x_N})^T \tag{13b}$$

with

$$p = \sin \alpha / c_0, \tag{13c}$$

where ω is the radial frequency, c_0 the velocity just below the surface, and α the emergence angle of the plane wave.

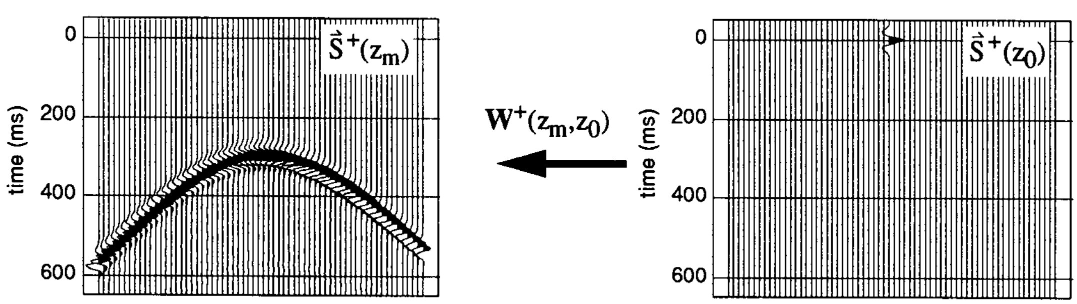

FIG. 3. The time-domain representation of the source wavefield at the surface (right) and at the target depth (i.e., 500 m, left). Notice the asymmetry in the incident source wavefield at depth level z_m due to the inhomogeneities of the overburden (Figure 2). Also note the 45-degree phase shift in the wavelet due to the line source assumption of the 2-D finite-difference scheme.

However, using knowledge of the overburden it is possible to design the synthesis operator $\Gamma^+(z_0)$ in such a way that the incident wavefield at depth level z_m is a prespecified wavefield describing the optimum illumination of the target zone below z_m. For example, we could arbitrarily allow unit amplitude and vertical incidence at every lateral position at the top of the target. Taking into account the propagation effects in the overburden during synthesis is the essence of our method.

The design of the synthesis operator

To design the synthesis operator $\Gamma^+(z_0)$, we have to define a desired wavefield $\mathbf{S}^+_{\text{syn}}(z_m)$ at depth level z_m. Then by inverting equation (12), the synthesis operator $\Gamma^+(z_0)$ follows:

$$\Gamma^+(z_0) = [\underline{\mathbf{S}}^+(z_0)]^{-1}\underline{\mathbf{F}}^+(z_0, z_m)\mathbf{S}^+_{\text{syn}}(z_m), \quad (14)$$

where $\underline{\mathbf{F}}^+(z_0, z_m)$ is the inverse of the propagation operator $\underline{\mathbf{W}}^+(z_m, z_0)$. Note that $[\underline{\mathbf{S}}^+(z_0)]^{-1}$ means correction for the individual sources (deconvolution for signature and directivity).

If we assume that the deconvolution process for the directivity has already been applied, then we may write:

$$\underline{\mathbf{S}}^+(z_0) = S(\omega)\underline{\mathbf{I}}, \quad (15)$$

where $\underline{\mathbf{I}}$ is the unity matrix, simplifying equation (14) to:

$$\Gamma^+(z_0) = [S(\omega)]^{-1}\underline{\mathbf{F}}^+(z_0, z_m)\mathbf{S}^+_{\text{syn}}(z_m). \quad (16)$$

Next we define the desired source wavefield $\mathbf{S}^+_{\text{syn}}(z_m)$ as:

$$\mathbf{S}^+_{\text{syn}}(z_m) = S(\omega)\Gamma^+(z_m). \quad (17)$$

Substitution of equation (17) into equation (16) yields:

$$\Gamma^+(z_0) = \underline{\mathbf{F}}^+(z_0, z_m)\Gamma^+(z_m). \quad (18)$$

As mentioned before, the inverse propagation operator $\underline{\mathbf{F}}^+(z_0, z_m)$ can be approximated by the complex conjugate of the propagation operator $\underline{\mathbf{W}}^-(z_0, z_m)$, see e.g., Wapenaar and Berkhout (1989), simplifying equation (18) to:

$$\Gamma^+(z_0) = [\underline{\mathbf{W}}^-(z_0, z_m)]^*\Gamma^+(z_m). \quad (19)$$

So synthesis operator $\Gamma^+(z_0)$ is defined as the areal source wavefield $\Gamma^+(z_m)$ propagated back to the surface z_0. Hence, synthesis operator $\Gamma^+(z_0)$ can be constructed from the desired wavefield at the target, if the macro model is known. Note the relationship between the synthesis operators and synthesized wavefields:

$$\mathbf{S}^+_{\text{syn}}(z_m) = S(\omega)\Gamma^+(z_m), \text{ and } \mathbf{S}^+_{\text{syn}}(z_0) = S(\omega)\Gamma^+(z_0). \quad (20)$$

If we define our desired source wavefield $\mathbf{S}^+_{\text{syn}}(z_m)$ at the target as shown in Figure 5 (right), the synthesis operator $\Gamma^+(z_0)$ appears as shown in Figure 5 (left). Note that the synthesis operator is designed in such a way that the incident wavefield will arrive at depth level z_m at $t = 0$.

It is important to realize that the handling of multi arrival time synthesis operators is automatically taken care of in the frequency domain.

The application of the synthesis operator to the shot records

First recall the forward model, describing the data matrix after preinversion:

$$\underline{\mathbf{P}}^-(z_0) = [\underline{\mathbf{W}}^-(z_0, z_m)\underline{\mathbf{X}}(z_m, z_m)\underline{\mathbf{W}}^+(z_m, z_0)]\underline{\mathbf{S}}^+(z_0), \quad (21a)$$

or, assuming $\underline{\mathbf{S}}^+(z_0) = S(\omega)\underline{\mathbf{I}}$,

$$\underline{\mathbf{P}}^-(z_0) = \underline{\mathbf{X}}(z_0, z_0)S(\omega), \quad (21b)$$

with

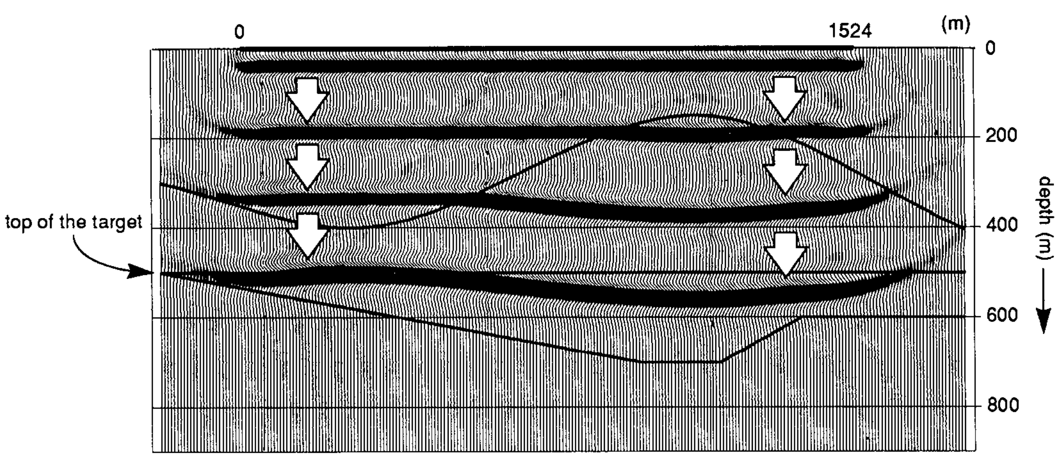

FIG. 4. Propagation of a plane wave through the overburden to the top of the target. This plane wave is constructed via conventional synthesis of point sources at the surface. Here a horizontal plane wave was chosen. Note the undesired diffraction tails due to the finite aperture of the areal source at the surface, and the undesired curvature of the wavefront at the target upper boundary, due to the inhomogeneities of the overburden.

$$\underline{X}(z_0, z_0) = \underline{W}^-(z_0, z_m)\underline{X}(z_m, z_m)\underline{W}^+(z_m, z_0). \quad (21c)$$

Applying the synthesis operator $\Gamma^+(z_0)$ to the data matrix $\underline{P}^-(z_0)$ we obtain:

$$\mathbf{P}^-_{syn}(z_0) = \underline{P}^-(z_0)\Gamma^+(z_0), \quad (22a)$$

or, according to equations (17), (18), and (21a),

$$\mathbf{P}^-_{syn}(z_0) = \underline{W}^-(z_0, z_m)\underline{X}(z_m, z_m)\mathbf{S}^+_{syn}(z_m), \quad (22b)$$

or

$$\mathbf{P}^-_{syn}(z_0) = \underline{X}(z_0, z_m)\mathbf{S}^+_{syn}(z_m), \quad (22c)$$

with

$$\underline{X}(z_0, z_m) = \underline{W}^-(z_0, z_m)\underline{X}(z_m, z_m). \quad (22d)$$

This result shows clearly that $\mathbf{P}^-_{syn}(z_0)$, as obtained by applying vector $\Gamma^+(z_0)$ to $\underline{P}^-(z_0)$, is the response at the surface z_0 due to the desired source wavefield at depth level z_m. The result of the application of the synthesis operator $\Gamma^+(z_0)$ to the data matrix $\underline{P}^-(z_0)$, yielding one areal shot record, is shown in Figure 6 for the situation of a plane wave at z_m:

$$\mathbf{S}^+_{syn}(z_m) = S(\omega)[1, 1, 1, \ldots, 1]^T.$$

In the time domain, this synthesis process can be explained as follows. Each shot record of Figure 6 (left) is convolved by one trace of Figure 5. Subsequently, the resulting shot records are stacked per common receiver, yielding the synthesized result in Figure 6.

Redatuming after synthesis

To obtain the redatumed areal shot record at depth level z_m due to the desired source wavefield $\mathbf{S}^+_{syn}(z_m)$, the propagation effects that the overburden has on the received wavefield must be removed by inverting for $\underline{W}^-(z_0, z_m)$:

$$\mathbf{P}^-_{syn}(z_m) = \underline{F}^-(z_m, z_0)\mathbf{P}^-_{syn}(z_0). \quad (23)$$

Upon substitution of equation (22b), we obtain:

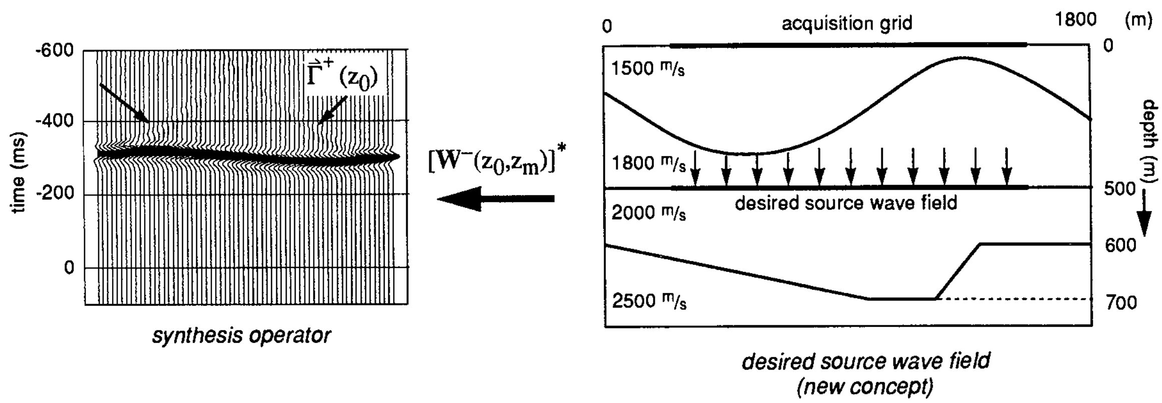

FIG. 5. Time-domain representation of the designed synthesis operator $\Gamma^+(z_0)$. Note that the diffractions in $\Gamma^+(z_0)$ are needed to avoid them in $\mathbf{S}^+_{syn}(z_m)$. In this simple example, a horizontal plane wave at depth level z_m was chosen. For display purposes the synthesis operator is convolved with the wavelet of Figure 2.

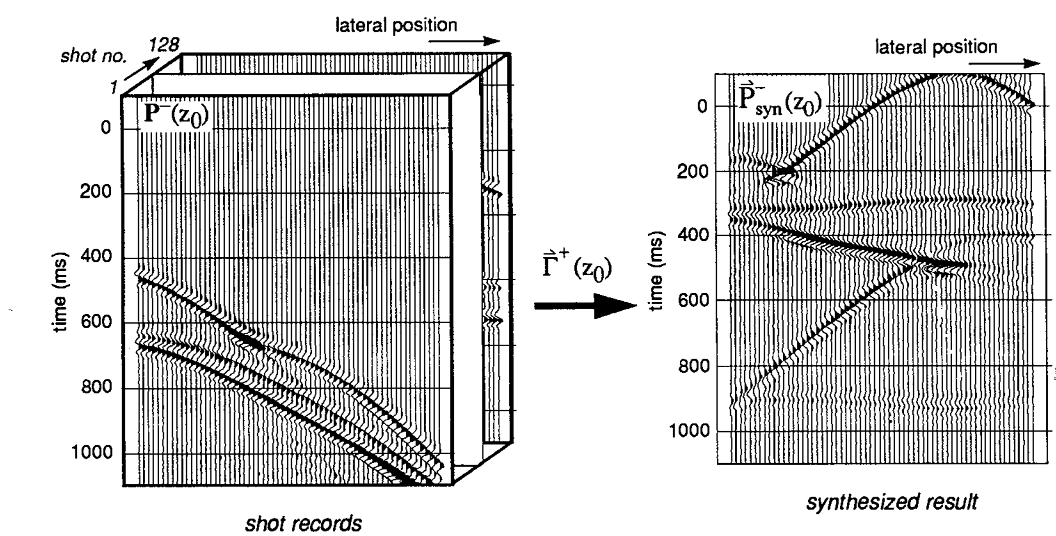

FIG. 6. Application of the synthesis operator $\Gamma^+(z_0)$ to the data, yielding one areal shot record. In the synthesized result, the source is a plane-wave source at $z = 500$ m (Figure 5); the receivers are at the surface.

$$\mathbf{P}^{-}_{\text{syn}}(z_m) = \underline{\mathbf{X}}(z_m, z_m)\mathbf{S}^{+}_{\text{syn}}(z_m). \tag{24}$$

The result is depicted in Figure 7 and shows the response at depth level z_m due to the desired source wavefield $\mathbf{S}^{+}_{\text{syn}}(z_m)$. Note again that the extrapolation, as described by equation (23), is done for only one synthesized areal shot record instead of all individual shot records, thus speeding up the calculations by a factor of the order of the number of shots! The structure in the target can be clearly seen after migration of the redatumed response, Figure 8.

Finally, Figure 9 shows a migrated areal shot record for all depth levels. Note that due to the limited acquisition aperture some artifacts are visible at the right-hand edge of the section. For details the reader is referred to Berkhout (1992).

Comparison with conventional redatuming

For a comparison with the conventional redatuming scheme, as described in the section Prestack redatuming, we substitute equation (8) into equation (24):

$$\mathbf{P}^{-}_{\text{syn}}(z_m) = [\underline{\mathbf{F}}^{-}(z_m, z_0)\underline{\mathbf{X}}(z_0, z_0)\underline{\mathbf{F}}^{+}(z_0, z_m)]\mathbf{S}^{+}_{\text{syn}}(z_m). \tag{25}$$

This shows, that synthesizing after redatuming [equation (25)] is fully equivalent to synthesizing sources at the surface in the sense of equation (22a) and extrapolating the receivers afterwards, according to equation (23). Hence no accuracy is lost. It may also be stated here, that no assumption whatsoever is made on the form of the desired source wavefield $\mathbf{S}^{+}_{\text{syn}}(z_m)$. This vector may have any form, thus describing any desired illumination of the reservoir. Figure 10 shows the result of the synthesis before and after redatuming. The resemblance confirms our theoretical expectation.

Illumination of a curved reflector

In the next example, we will use the same model shown in Figure 2. However, instead of a plane-wave illumination, this time the third reflector will be illuminated in a normal incidence way, to show the flexibility of the method with respect to the type of illumination.

First the synthesis operator is calculated (Figure 11). Application of the synthesis operator to the data matrix leads to the areal shot record as depicted in Figure 12. This areal shot record is the response at the surface due to the prespecified areal source at the third boundary of the model. After extrapolation of the receivers, we are left with the redatumed response, Figure 13. Although the redatuming level has a complicated shape, it can be clearly seen that the redatumed response has only one event at $t = 0$ for every lateral position, thus showing that the third boundary is perfectly illuminated.

THE INFLUENCE OF MISSING DATA

In the previous examples, a fixed spread acquisition was used, thus filling the data matrix completely. In practice, however, a moving spread acquisition is used, making a

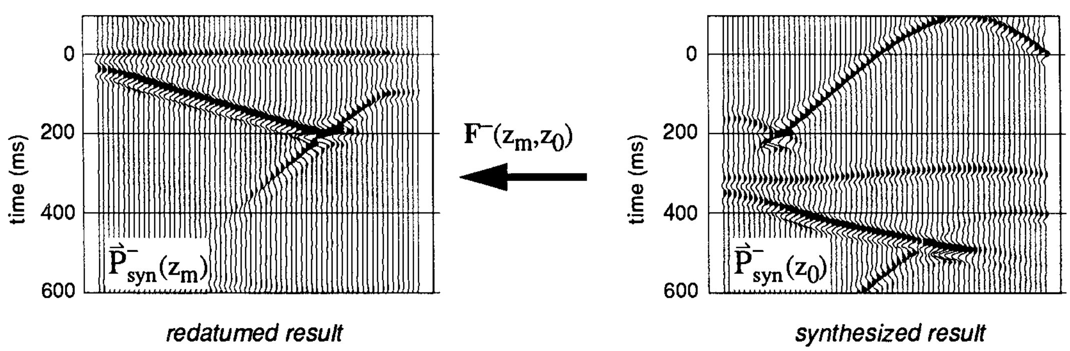

FIG. 7. The synthesized response after downward extrapolation, meaning that the receivers are repositioned from z_0 to z_m.

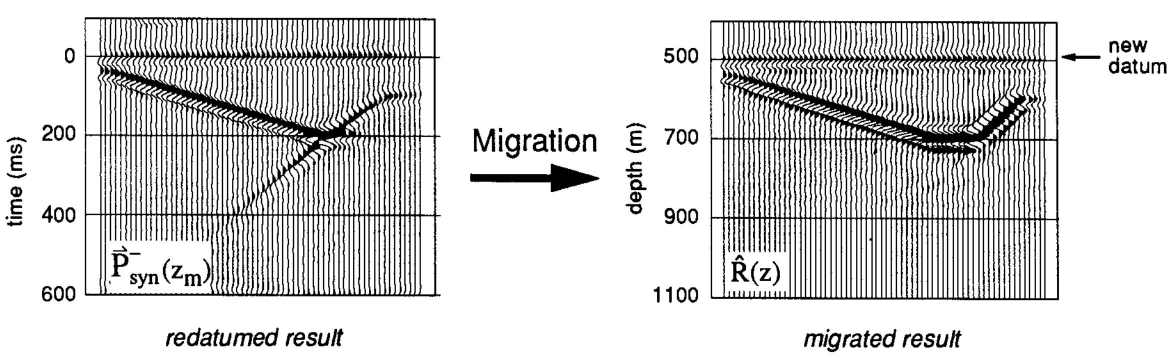

FIG. 8. Migration of the downward extrapolated synthesized response.

band data matrix (Figure 14). The most simple solution to the problem of processing a band data matrix is to process this matrix as if it was a full data matrix. To do so, one should append zeros to the band data matrix, thus filling the data matrix completely.

After synthesis, this processing option leaves one areal shot record, with a spread of receivers equal to the total spread of the acquisition grid at the surface. With this method, all recorded data is used and a maximum data reduction is achieved.

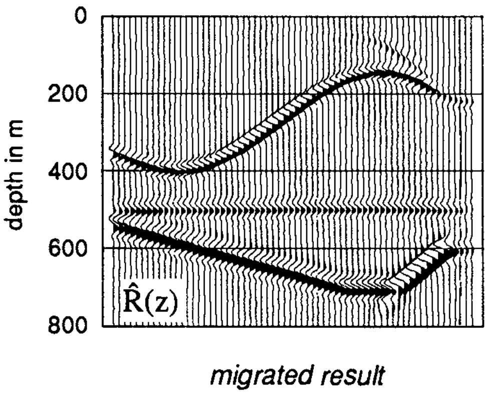

FIG. 9. Fully migrated areal shot record, obtained by migration of the areal shot record as shown in Figure 6 for all depth levels.

Example

In this example, the same model is used as before (Figure 2). Now a moving split spread acquisition is used, consisting of 64 source surface positions with each 65 receivers (Figure 14). For the desired source wavefield, a normal incidence plane-wave illumination was chosen at z_m with a lateral spreading at the top of the target equal to the lateral spread of all surface source positions, as shown in Figure 15.

First the synthesis operator is calculated. The synthesis operator as shown in Figure 15 clearly shows the desired diffraction tails due to the limited aperture of the desired source wavefield at the target. Because the synthesis operator is applied to the shot records, only the middle part of the synthesis operator will be used in this case due to the limitation of the acquisition aperture. Application of the synthesis operator to the band data matrix leads to the result depicted in Figure 16. This result is the response of the target at the surface due to the prespecified areal source at the second boundary of the model. After extrapolation of the received wavefield, we are left with the redatumed response in Figure 17. Here we see that the middle part of the second reflector is perfectly illuminated, although the data matrix was only partly filled. The migrated section (Figure 18), shows the structure of the reservoir within the range of the predefined areal source perfectly. Note that only a quarter of the total amount of data is used, in comparison with the example as shown in Figure 8 where a full data matrix was used.

(Continued on p. 1345)

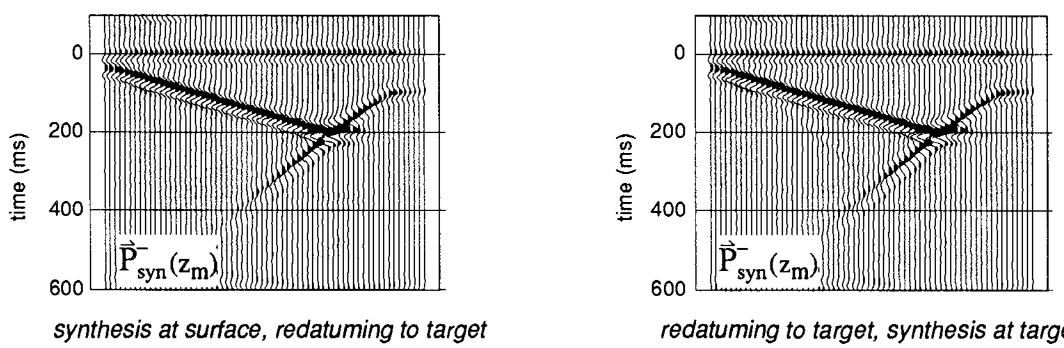

FIG. 10. The result of synthesis before and after redatuming.

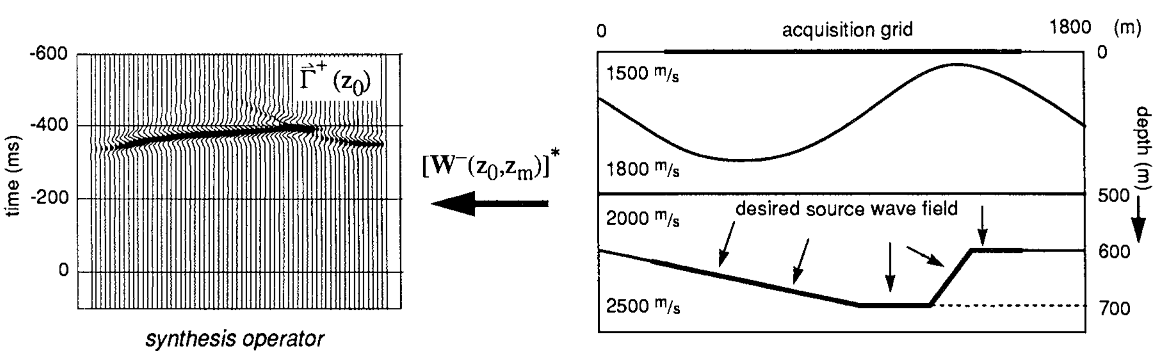

FIG. 11. The calculated synthesis operator according to the defined illumination and the macro model. For display purposes, the synthesis operator is convolved with the wavelet of Figure 2.

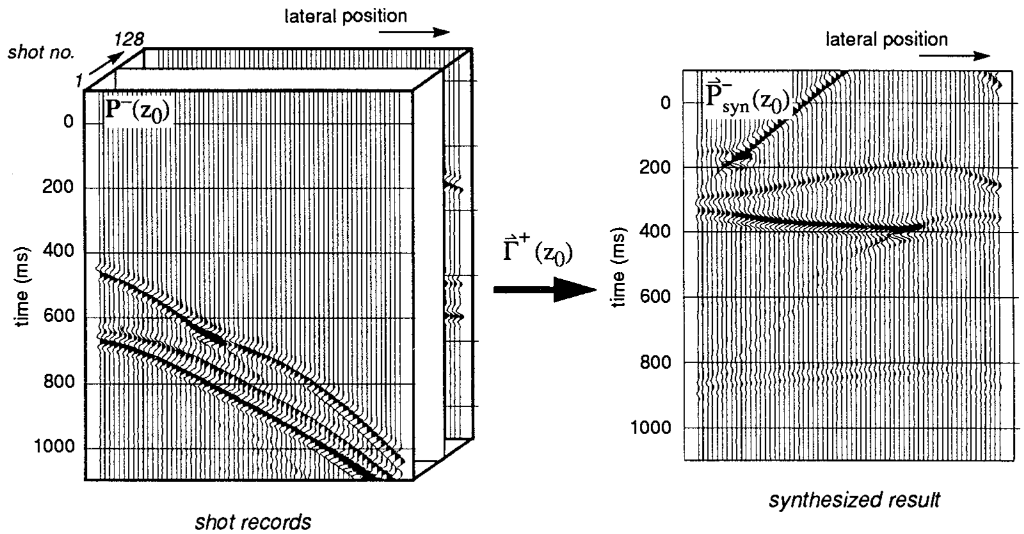

FIG. 12. Application of the synthesis operator to the data, yielding one areal shot record.

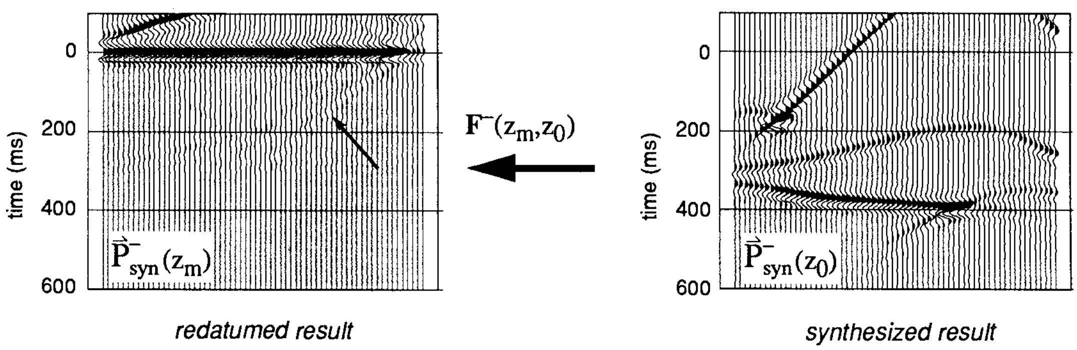

FIG. 13. The synthesized response after downward extrapolation of the received wavefield. Since the diffraction energy from the target boundary is not entirely present in the surface data, the redatumed result shows some truncation artifacts indicated by the arrow.

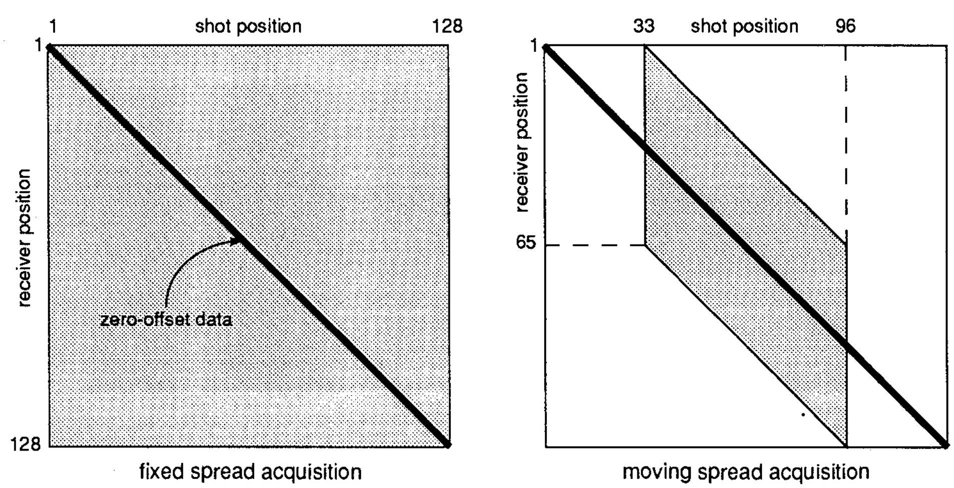

FIG. 14. Influence of the acquisition on the form of the data matrix. On the left-hand side, the full data matrix is shown as used in the examples of Figures 5–13. On the right-hand side the data matrix is shown as used in the example of Figures 15–18. Note that only a quarter of the total amount of data is used.

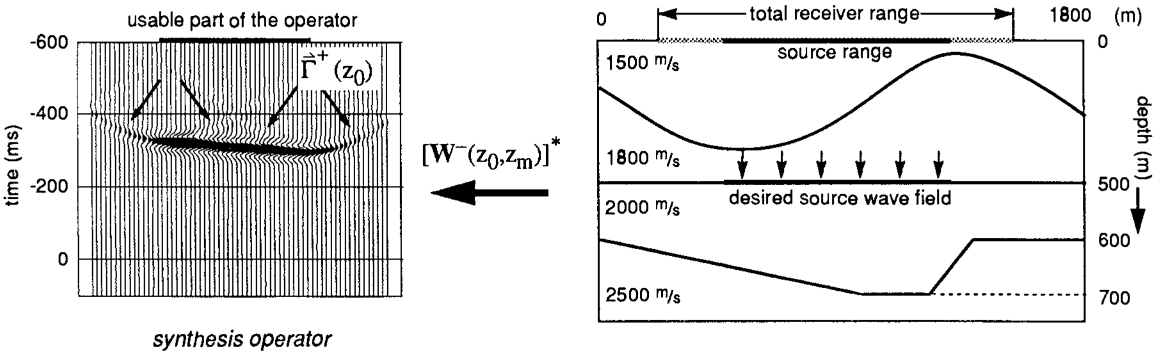

FIG. 15. The calculated synthesis operator $\Gamma^+(z_0)$ according to the defined illumination and the macro model. The source range indicates the range of all surface positions of the 64 sources. The receiver range indicates the total range of all 128 receiver positions. Per shot, 65 receivers were used in a moving, split spread configuration (Figure 14). In the operator, the usable part is indicated: outside this range no shots are available in this experiment. The arrows indicate the diffraction tails due to the limited width of the desired source wavefield. The diffractions in the synthesis operator are needed to avoid diffraction tails in the final, redatumed result. For display purposes, the synthesis operator is convolved with the wavelet of Figure 2.

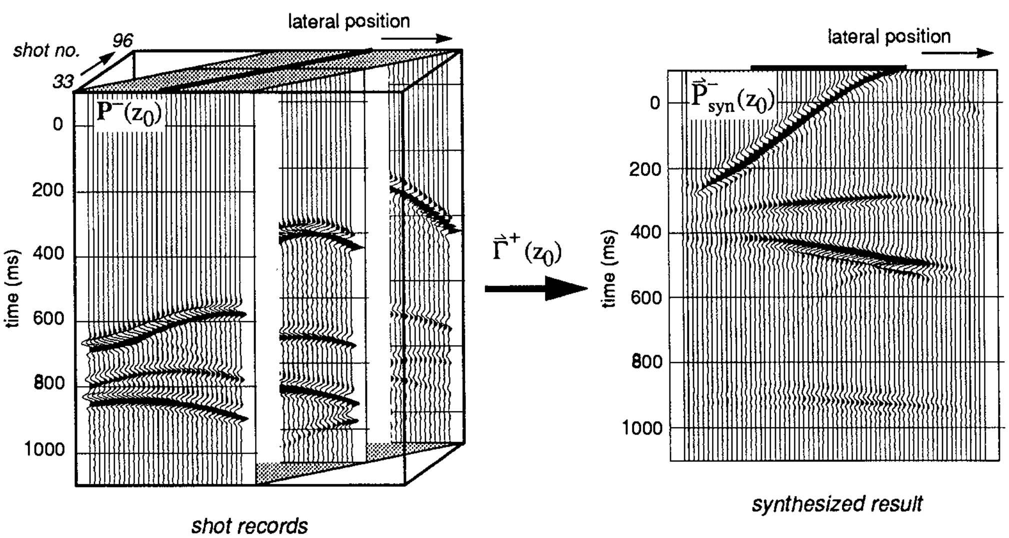

FIG. 16. Application of the synthesis operator $\Gamma^+(z_0)$ to the data. Note that due to the missing far offsets, the data matrix is represented by a band data matrix.

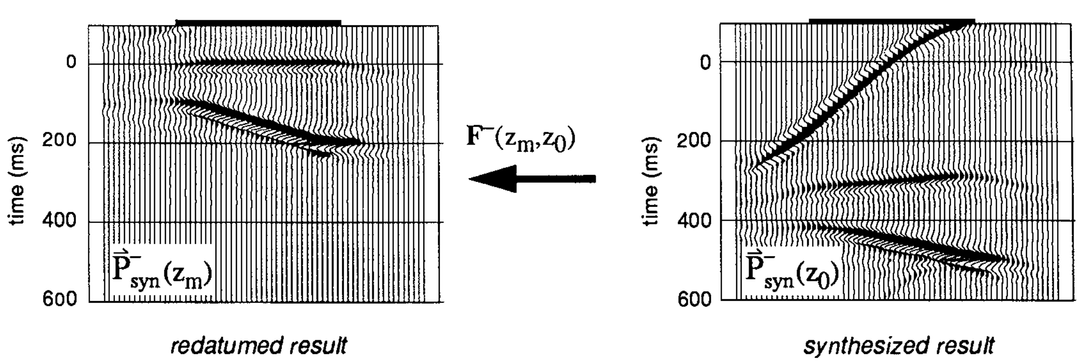

FIG. 17. The synthesized response after downward extrapolation, meaning that the receivers are repositioned from z_0 to z_m.

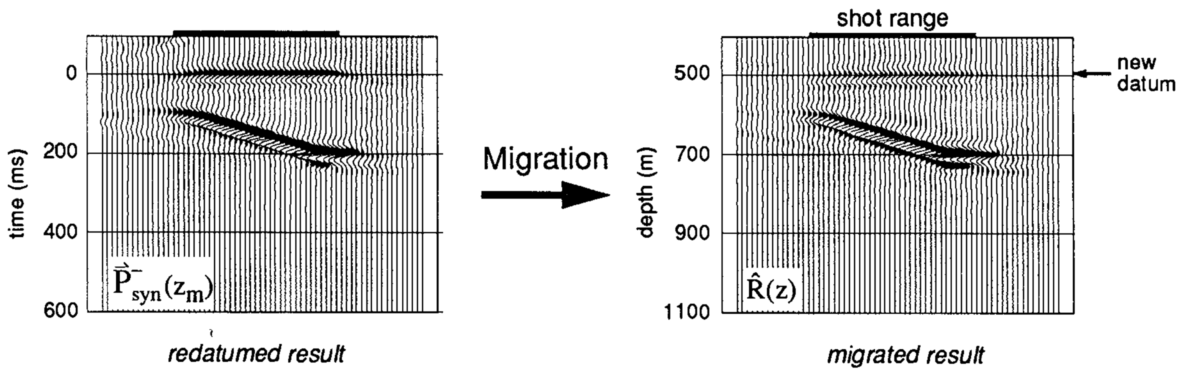

FIG. 18. Migration of the downward extrapolated synthesized response.

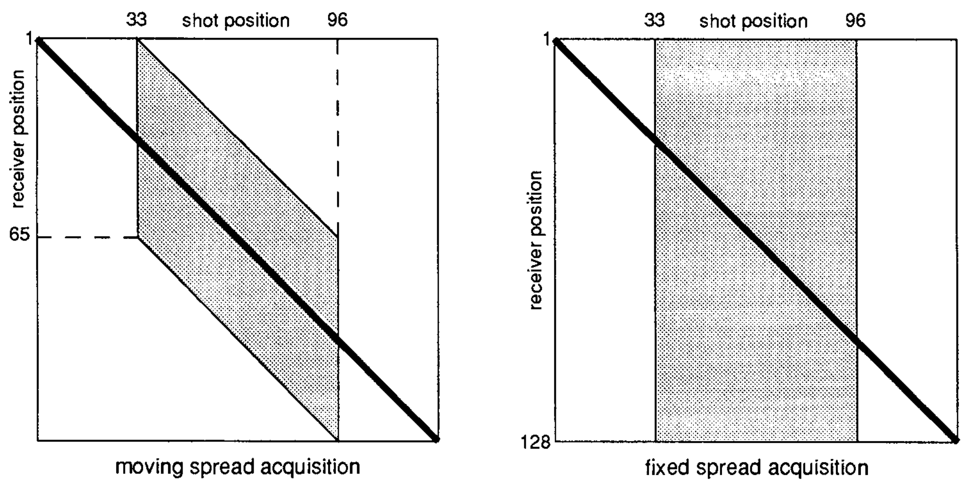

FIG. 19. Acquisition used for the experiment with moving spread acquisition (left), and the fixed spread acquisition (right), both with the same shot range.

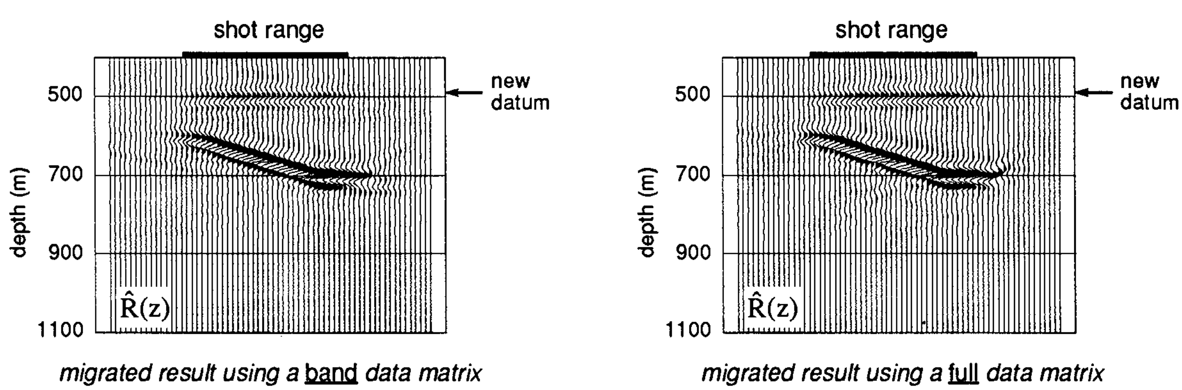

FIG. 20. Migrated sections of the downward extrapolated synthesized responses, using a band data matrix at the left-hand side, and a full data matrix (i.e., for all used shots, all receiver positions were used) at the right-hand side. The same shot range was used in both experiments. Only minor differences can be noticed.

For comparison the same experiment was performed with a full data matrix, i.e., a fixed spread of 128 receivers over the same shot range of 64 surface positions (Figure 19). Figure 20 shows the migrated result together with the migrated result as already shown in Figure 18. The results match very well within the shot range used.

In conclusion, the example indicates that the proposed method does not break down in case of an incomplete data matrix. The structural information from the reservoir under investigation is still revealed perfectly. The important issue of obtaining true amplitude results when working with an incomplete data matrix is still under investigation.

CONCLUSIONS

If $\mathbf{S}^+_{\text{syn}}(z_m)$ is the desired source wavefield at z_m, then the synthesis operator $\mathbf{\Gamma}^+(z_0)$ at the surface is computed by:

$$\mathbf{\Gamma}^+(z_0) = [\underset{\sim}{\mathbf{W}}^-(z_0, z_m)]^* \mathbf{\Gamma}^+(z_m), \tag{26}$$

where $\mathbf{\Gamma}^+(z_m)$ represents $\mathbf{S}^+_{\text{syn}}(z_m)$ for a unit source function.

Note that in conventional synthesis the control of the source wavefield is not put at the target but is put at the surface, meaning that $\mathbf{\Gamma}^+(z_0)$ is specified instead of $\mathbf{\Gamma}^+(z_m)$.

The actual synthesis process involves a weighted common receiver stacking in the frequency domain, the weighting factors being the complex valued elements of synthesis vector $\mathbf{\Gamma}^+(z_0)$:

$$\mathbf{P}^-_{\text{syn}}(z_0) = \underset{\sim}{\mathbf{P}}^-(z_0)\mathbf{\Gamma}^+(z_0). \tag{27}$$

Therefore a considerable data reduction is achieved (by a factor of the number of channels), speeding up the subsequent processing time significantly. Redatuming to the target now simply involves downward extrapolation of the synthesized shot record:

$$\mathbf{P}^-_{\text{syn}}(z_m) = [\underset{\sim}{\mathbf{W}}^+(z_m, z_0)]^* \mathbf{P}^-_{\text{syn}}(z_0). \tag{28}$$

The total procedure, as defined by equations (26)–(28), fully preserves the amplitude information of the target response. It is also shown that the result of the process "synthesis at the surface followed by redatuming to the target" is identical to the result of the process "redatuming to the target followed by synthesis at the target."

It is shown that good results are also obtained by the method if the data matrix is not entirely filled due to the use of a moving spread acquisition. The true amplitude issue related to missing data is still under investigation. The method is computationally fast due to the significant data reduction that is obtained by the synthesis: one synthesized result has the volume of a poststack section. This makes the application of the method to prestack 3-D data volumes very attractive and feasible.

Finally, due to the significant importance of the foregoing concept, we have now reformulated the full 3-D prestack migration theory in terms of a number of independent illumination steps.

ACKNOWLEDGMENT

We thank the members of the DELPHI consortium for their financial support and their stimulating comments.

REFERENCES

Berkhout, A. J., 1985, Seismic migration: Imaging of acoustic energy by wavefield extrapolation. A. Theoretical aspects, 3rd Ed.: Elsevier Science Publ. Co., Inc.

Berkhout, A. J., 1992, Areal shot record technology: J. Seis. Expl., **1**, no. 3.

Berkhout, A. J., and Wapenaar, C. P. A., 1990, DELPHI, Delft philosophy on acoustic and elastic inversion: The Leading Edge, **9**, No. 2, 30–34.

Berryhill, J. R., 1984, Wave-equation datuming before stack: Geophysics, **49**, 2064–2066.

Schultz, P. S., and Claerbout, J. F., 1978, Velocity estimation and downward continuation by wavefront synthesis: Geophysics, **43**, 691–714.

Taner, M. T., 1976, Simplan: simulated plane-wave exploration: 46th Ann. Internat. Mtg., Soc. Expl. Geophys., Expanded Abstracts, 186–187.

Verschuur, D. J., Berkhout, A. J., and Wapenaar, C. P. A., 1992, Surface-related multiple elimination: Geophysics, **57**, 1166–1177.

Wapenaar, C. P. A., and Berkhout, A. J., 1989, Elastic wavefield extrapolation: Redatuming of single- and multicomponent seismic data: Elsevier Science Publ. Co., Inc.